J|A|C|S COMMUNICATIONS

Published on Web 08/19/2009

An Efficient Route to Highly Organized, Tunable Macroporous−Mesoporous Alumina

Jean-Philippe Dacquin,[†] Jérémy Dhainaut,[†] Daniel Duprez,[‡] Sébastien Royer,[‡] Adam F. Lee,*[,†,§] and Karen Wilson*[,†]

Department of Chemistry, University of York, Heslington, York YO10 5DD, U.K., and Université de Poitiers, LACCO UMR 6503 CNRS, 40 Avenue du Recteur Pineau, 86022 Poitiers Cedex, France

Received July 9, 2009; E-mail: afl2@york.ac.uk; kw13@york.ac.uk

The preparation of bimodal porous materials incorporating two distinct pore networks spanning different scales is an important challenge for chemical applications including catalysis, sorption, and separation science. Since the parallel development of mesostructuring[1] and macrostructuring[2,3] routes in the 1990s, the synthesis of hierarchical macroporous−mesoporous oxides has become an exciting area of materials chemistry. The first report of ordered macroporous−mesoporous silica[4] was followed by the discovery of numerous structuring agents able to direct macropore formation.[5,6] Considerable effort has been devoted to creating nonsiliceous analogues possessing *ordered* mesopores, but it has proven difficult to produce organized bimodal pore networks for such nonsiliceous solids. Indeed, the fast hydrolysis−condensation of aluminum generally leads to a wormhole-like mesopore,[7,8] and the stabilization of a hexagonal mesopore array after calcination has rarely been reported.[9−12] Consequently, the transition from a pure mesoporous alumina to a bimodal macroporous−mesoporous one has only been achieved with disordered pore arrangements,[13−16] limiting control over the pore size and gross solid mass-transport properties. Alternative approaches, such as phase-separated bilayers of (nontemplated) mesoporous and macroporous alumina, suffer from heterogeneous pore size distributions and slow transport through the mesopore barrier layer.[17] Herein we report a simple and flexible method for obtaining a highly organized bimodal porous alumina via a dual-templating approach. This synthesis offers both tunable macroporosity and the formation of two well-defined pore networks. These characteristics make our new aluminas amenable to quantitative modeling of their mass transport properties and thus attractive candidates for catalyst supports in liquid-phase chemistry.

Synthetic details for all of the porous solids are provided in the Supporting Information. Briefly, a pure mesoporous alumina (Al-M) was prepared according to the evaporation-induced self-assembly procedure using Pluronic P123 triblock copolymer as a structuring agent, following Yuan et al.[11] This procedure yielded a well-resolved, hexagonal pore structure. To obtain macroporous−mesoporous solids, monodispersed latex spheres of controlled size (300 nm for Al-M300-M and 400 nm for Al-M400-M; see Figure S1 in the Supporting Information) were added to a solution containing the aluminum source and P123. The hybrid macro−mesophase was formed from the inorganic phase (aluminum isopropoxide), the structure-directing agent (P123), and the physical template via sedimentation of the polystyrene beads into a hexagonal or cubic close-packed array[18] followed by slow elimination of the supernatant solution. The resulting solids were calcined to remove the organic templates. This route is summarized in Figure S2. Our synthesis yielded organized mesoscopic and macroscopic assemblies. The final porous materials were fully characterized by N_2 porosimetry, thermal analysis, powder X-ray diffraction (XRD), transmission electron microscopy (TEM), and scanning electron microscopy (SEM).

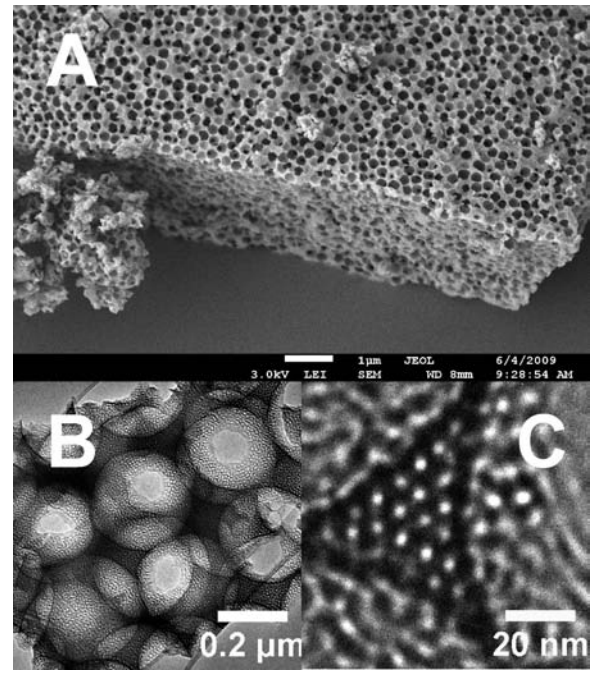

Figure 1. (A) SEM image obtained for the Al-M400-M sample; (B) low- and (C) high-magnification TEM images obtained for the Al-M400-M sample.

Electron microscopy reveals a high degree of network organization in all our aluminas. Micrographs for the pure mesoporous alumina (Figure S3) show the hexagonal arrangement of pores throughout the solid. Representative images for Al-M400-M and Al-M300-M samples are shown in Figure 1 and Figure S4a,c, respectively.

SEM highlights the strong, long-range structural ordering imparted by the polystyrene template (subsequently removed during calcination), which resulted in the regular macroporous skeleton seen in Figure 1A. It is interesting to note that the diameter of the macropores (320 nm; Table 1) is ∼20% smaller than that of the 400 nm PS beads used in their synthesis. Likewise the Al-M300-M sample possesses macropores with a diameter of 212 nm (Table 1, Figure S4a) derived from 300 nm PS beads during the synthesis.

TEM directly visualizes the macropore network (Figure 1B and Figure S4a,b) and furthermore reveals the extended mesoscopic ordering resulting from self-assembly of the block copolymer solution (Figure 1C, Figure S4c). Indeed, the macroporous frame-

[†] University of York.
[‡] Université de Poitiers, LACCO UMR 6503 CNRS.
[§] Present address: School of Chemistry, Cardiff University.

10.1021/ja9056486 CCC: $40.75

Table 1. Physical and Structural Properties of Selected Mesoporous and Macroporous−Mesoporous Samples

sample	S_{BET} (m^2 g^{-1})[a]	$D_{mesopore}$ (nm)[b]	$V_{mesopore}$ (cm^3 g^{-1})[c]	$D_{macropore}$ (nm)[d]	d_{100} (nm)[e]	wall thickness (nm) [f]	crystal phase
Al-M	259	5.8	0.54	−	9.5	5.2	none
Al-M300-M	249	5.1	0.49	212	9.7	6.1	none
Al-M400-M	207	4.0	0.40	320	9.9	7.5	none

[a] Specific surface area obtained from adsorption data in the range $0.07 < P/P_0 < 0.30$. [b] Mesopore diameter taken at the middle of the segment defined by the peak width at half height (BJH pore size distribution). [c] Mesopore volume evaluated for $P/P_0 > 0.980$. [d] Average macropore diameter obtained using TEM. [e] Interplanar spacing determined from Bragg's law. [f] Wall thickness calculated for a hexagonal system $= (2d_{100}/\sqrt{3}) - D_{mesopore}$.

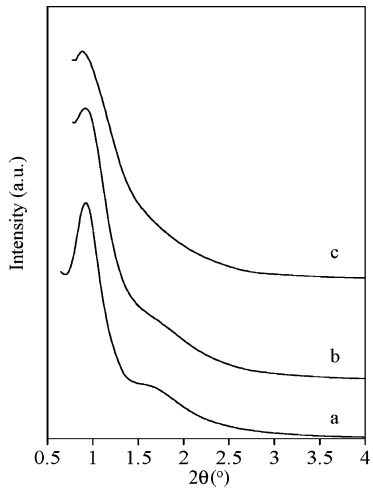

Figure 2. Low-angle XRD patterns obtained for the mesostructured alumina Al-M (a) and the two macro−mesostructured solids Al-M300-M (b) and Al-M400-M (c).

work clearly comprises well-defined channels arising from ordered, hexagonally packed mesopores (Figure 1C and Figure S4b,c). As discussed in the literature,[19] the mesopore network may be perturbed by the interpenetrating spherical macropores, which inevitably place geometric constraints on hexagonal cells within the mesopore network in macroporous−mesoporous solids. Notably, the macrostructure cell contraction seen during calcination does not influence the associated macropore periodicity.

Low-angle powder XRD confirms the genesis of an ordered mesophase (Figure 2). Our reference Al-M sample exhibits a well-defined reflection at 0.93° with an additional broad peak at ∼1.6° characteristic of (100) and (110)/(200) planes in materials exhibiting *p6mm* hexagonal symmetry.[11] Similar features were observed for our two macroporous−mesoporous variants. Despite attenuated reflections, which we attribute to the macropore-induced strain and distortions mentioned above, the corresponding d_{100} (Table 1) and lattice parameters are extremely close to those for the Al-M reference. TEM and XRD thus provide unequivocal evidence for the first macroporous aluminas also possessing long-range mesoscopic order.

Wide-angle XRD patterns spanning 20−80° reveal no evidence of crystalline alumina phases (Figure S5). This suggests that the framework comprises alumina transitional between hydroxide or oxyhydroxide (as seen in some macroporous aluminas hydrothermally or microwave-synthesized at 500 °C) and γ-Al_2O_3, which only crystallizes at higher calcination temperatures (>700 °C)[11] than employed in this study. Such transitional aluminas are particularly interesting from a catalytic perspective, since their defective nature can help stabilize isolated transition-metal centers, giving rise to "single-site" heterogeneous catalysts.[20]

In addition to their high degree of order, these aluminas possess surface areas and mesopore dimensions similar to those of pure mesoporous alumina (Table 1). The incorporation of macropores only slightly perturbs the isotherm shown in Figure S6A, which remains of type IV (characteristic of a mesoporous solid), albeit with reduced mesopore volume. The corresponding pore size distributions shown in Figure S6B are also narrow, consistent with the regular pores seen by TEM, while the surface areas are higher than for either commercial γ-alumina or macroporous Al_2O_3 from previous syntheses.[21,22] Our materials are robust and thermally stable up to 800 °C (Figure S7) and amenable to simple multigram production.

The combination of high surface area, thick-walled *ordered mesopores*, and very uniform macropores paves the way to new alumina supports that have predictable diffusion characteristics and are ideal for functionalization by metal nanoparticles and application in liquid/gas-phase catalysis.

Acknowledgment. We thank the Engineering and Physical Sciences Research Council for financial support (EP/F063423/1; EP/G007594/1) and the award of a Leadership Fellowship (A.F.L.). We thank Serge Kaliaguine and Sébastien Vaudreuil (Laval University) for advice on latex bead synthesis.

Supporting Information Available: Detailed materials synthesis and characterization. This material is available free of charge via the Internet at http://pubs.acs.org.

References

(1) Kresge, C. T.; Leonowicz, M. E.; Roth, W. J.; Vartuli, J. C.; Beck, J. S. *Nature* **1992**, *359*, 710.
(2) Imhof, A.; Pine, D. J. *Nature* **1997**, *389*, 948.
(3) Holland, B. T.; Blanford, C. F.; Stein, A. *Science* **1998**, *281*, 538.
(4) Yang, P.; Deng, T.; Zhao, D.; Feng, P.; Pine, D.; Hekla, B. F.; Whitesides, G. M.; Stucky, G. D. *Science* **1998**, *282*, 2244.
(5) Antonelli, D. M. *Microporous Mesoporous Mater.* **1999**, *33*, 209.
(6) Vaudreuil, S.; Bousmina, M.; Kaliaguine, S.; Bonneviot, L. *Adv. Mater.* **2001**, *13*, 1311.
(7) Bagshaw, S. A.; Prouzet, E.; Pinnavaia, T. J. *Science* **1995**, *269*, 1242.
(8) Zhang, W.; Pinnavaia, T. J. *Chem. Commun.* **1998**, 1185.
(9) Yang, P.; Zhao, D.; Margolese, D. I.; Chmelka, B. F.; Stucky, G. D. *Nature* **1998**, *396*, 152.
(10) Niesz, K.; Yang, P.; Somorjai, G. A. *Chem. Commun.* **2005**, 1985.
(11) Yuan, Q.; Yin, A.-X.; Luo, L.-D.; Zhang, Y.-W.; Duan, W.-T.; Liu, H.-C.; Yan, C.-H. *J. Am. Chem. Soc.* **2008**, *130*, 3465.
(12) Morris, S. M.; Fulvio, P. F.; Jaroniec, M. *J. Am. Chem. Soc.,* **2008**, *130*, 15210.
(13) Blin, J.-L.; Leonard, A.; Yuan, Z.-Y.; Gigot, L.; Vantomme, A.; Cheetham, A. K.; Su, B.-L. *Angew. Chem., Int. Ed.* **2003**, *42*, 2872.
(14) Yuan, Z.-Y.; Ren, T.-Z.; Azioune, A.; Pireaux, J.-J.; Su, B.-L. *Chem. Mater.* **2006**, *18*, 1753.
(15) Deng, W.; Shanks, B. H. *Chem. Mater.* **2005**, *17*, 3092.
(16) Kim, Y.; Kim, C.; Yi, J. *Mater. Res. Bull.* **2004**, *39*, 2103.
(17) Gaikwad, A. V.; Vittorio, B.; ten Elshof, J. E.; Rothenberg, G. *Angew. Chem., Int. Ed.* **2008**, *47*, 5407.
(18) Vos, W. L.; Megens, M.; Van Kats, C. M.; Böseke, P. *Langmuir* **1997**, *13*, 6004.
(19) Sel, O.; Kuang, D.; Thommes, M.; Smarsly, B. *Langmuir* **2006**, *22*, 2311.
(20) Hackett, S. F. J.; Brydson, R. M.; Ghass, M. H.; Harvey, I.; Newman, A. D.; Wilson, K.; Lee, A. F. *Angew. Chem., Int. Ed.* **2007**, *46*, 8593.
(21) Holland, B. T.; Blanford, C. F.; Do, T.; Stein, A. *Chem. Mater.* **1999**, *11*, 795.
(22) Li, H.; Zhang, L.; Dai, H.; He, H. *Inorg. Chem.* **2009**, *48*, 4421.

JA9056486